PERGAMON

Control Engineering Practice 8 (2000) 861–871

CONTROL ENGINEERING PRACTICE

www.elsevier.com/locate/conengprac

Sliding mode control of a large flexible space structure

Matthew Allen[a], Franco Bernelli-Zazzera[b,*], Riccardo Scattolini[a]

[a]*Dipartimento di Informatica e Sistemistica, Università degli Studi di Pavia, Via Ferrata 1, 27100 Pavia, Italy*
[b]*Dipartimento di Ingegneria Aerospaziale, Politecnico di Milano, Via La Masa 34, 20158 Milano, Italy*

Received 17 October 1997; accepted 10 September 1999

Abstract

This paper presents an experimental study on active vibration control of a flexible structure. The control uses constant force air-jet thrusters as actuators, and the switching logic is designed using the theory of sliding mode control. The design of the sliding surface for the system is based on a quadratic criterion involving the first six natural modes of the structure. It allows the system response to be shaped and the relative importance of the control of each mode to be defined with respect to the control power available. Experimental results were found to be very satisfactory when compared with those obtained in previous studies on the same structure. To face the same disturbance, the control time is shorter and the residual speed smaller.

Keywords: Flexible structures; Non-linear control; Variable structure control; Vibration control

1. Introduction

The evolution of the topology and mechanical characteristics of space structures over the past two decades has been so peculiar that it has given rise to a distinct category of structures, called large-space structures (LSS). They are characterised by the presence of numerous natural vibration modes within the control and disturbance bandwidth. Therefore, without active control, these structures tend to be unacceptably disturbed, compromising the optimal performances of antennas, solar panels and any other pointing instrument. In this context, active control of a LSS becomes mandatory, and can be considered a mature research field (Junkins, 1990) with many experimental results available (Sparks & Juang, 1992). It represents a challenging and interesting field of research because, to be effectively applied in the space environment, a control system must be simple, reliable and performing. Bang–bang techniques are rather simple to implement and their major interest is related to the extreme simplicity and well-proven affordability of the hardware required to perform the control. Jet thrusters of different specific impulses and sizes have regularly been used for attitude control, and their adoption in vibration suppression problems appears to be promising. However, experience has shown that simple control switching strategies, such as the direct velocity feedback control, do not guarantee satisfactory performances (Hallauer & Lamberson, 1989). Improvements of this control strategy have been proposed and experimentally verified (Casella, Locatelli & Schiavoni, 1996), where a modified velocity feedback has been used. However, the method does not consider the presence of rigid body modes and the tuning of its parameters is strictly dependent on the particular structure. In general, devices capable of modulating the control force should be used to achieve high performances. If this actuation is impossible or not wanted, the controller is very efficient in damping large disturbances, but lacks the capability of controlling small oscillations. In this case, sophisticated switching strategies must be adopted.

Among the numerous control techniques developed, preserving the simplicity of the on/off control action, variable structure control (VSC) or sliding mode control (SMC) techniques (Utkin, 1977) seem to offer most of the desirable features of a control algorithm for LSS. In fact, the resulting control is naturally robust with respect to uncertainties in the structural parameters and external disturbances. Moreover, SMC represents a systematic approach to the design of on/off control laws for multivariable systems.

* Corresponding author. Tel.: +39-02-2399-8328; fax: +39-02-2399-8334.

E-mail addresses: bernelli@aero.polimi.it (F. Bernelli-Zazzera), scatto@conpro.unipv.it (R. Scattolini).

0967-0661/00/$ - see front matter
PII: S0967-0661(00)00004-6

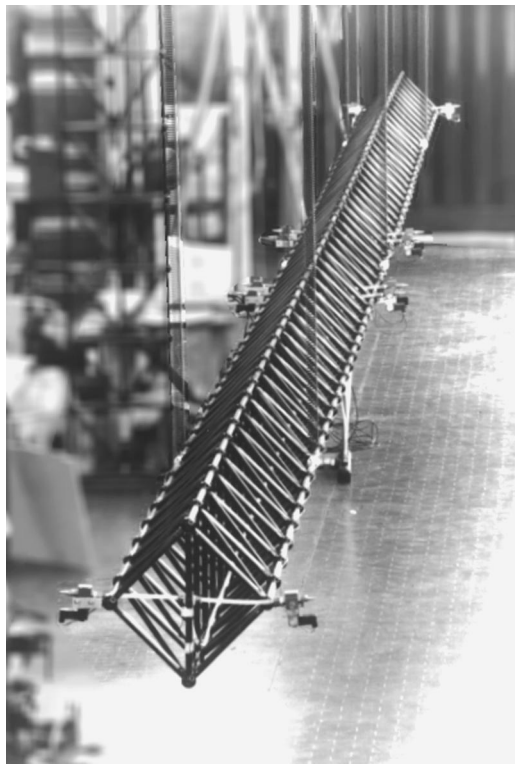

Fig. 1. The TESS experimental structure.

The theory of SMC has now been developed to the point that its robustness and performance are demonstrated on a wide variety of multi-input–multi-output (MIMO) systems. In principle, SMC consists of a control law that switches with infinite speed to drive the system on a specified state trajectory, called the sliding surface, and is capable of keeping the state on this surface. The control variable becomes the duration of a constant input, rather than its amplitude. Clearly, this type of control is intrinsically non-linear and falls into the broader class of pulse modulated control systems. One remarkable characteristic of SMC is that its design can be performed using analytical tools typical of linear systems. Aerospace applications of this technique have been studied, including those related to structural control (Dodds & Senior, 1993; Bernelli-Zazzera, 1995), but experiments in this field are lacking.

To fill the gap between theory and application, the objective of the present work is to study and verify the opportunities offered by SMC on a LSS available at the Politecnico di Milano (Ercoli-Finzi, Gallieni & Ricci, 1993), the truss experiment for space structures (TESS) experimental structure shown in Fig. 1. In particular, the various issues raised by the design of SM controllers have been analysed in detail. Among them, the most important are the design of the sliding surface and the reduction of the chattering phenomenon. It is believed that the results obtained in this application can also represent a useful guideline for the design of SM control algorithms for lightly damped flexible structures in general. Of particular interest is the experimental verification of SMC design on a structure subject to various disturbances and that naturally displays complex dynamics, most of which are unmodelled or simplified in the design of the controller. A direct comparison with the best results of a previous study (Casella et al., 1996) on the same structure will be discussed to highlight the advantages and disadvantages of the proposed controller.

2. Experimental set-up and mathematical model

2.1. Experimental device

The experimental space structure, shown in Fig. 1, is a modular truss having a mass of 75 kg and a length of 19 m, built with commercial PVC elements for a total of 54 cubic bays. The truss is suspended by three pairs of steel springs ensuring an acceptable uncoupling of rigid and elastic bending modes; it has been designed so that bending modes in the horizontal and in the vertical plane are independent, although closely spaced in frequency. This allows the controller to be designed and implemented in the horizontal plane only, without loss of generality.

The truss is equipped with six pairs of on–off air-jet thrusters (AJT). These actuators are mounted on the tips and near the middle of the structure as shown in Fig. 2. Actuator locations were chosen during a previous study and are considered as given and not subject to change. They maximise the controllability of the two rigid body modes and of the first four bending modes (Junkins, 1990).

The AJT actuators consist of electrovalves provided with convergent nozzles which can generate a transverse thrust of 2 N when supplied with air at 3 bar. Thrust is generated with a delay of about 12 ms after the transmission of the control command, and the actuators do not operate properly at switching frequencies greater than 40 Hz.

The horizontal motion of the structure is measured by four piezoresistive accelerometers positioned as shown in Fig. 2. The signals coming from these sensors are then processed by means of an analog filter, an A/D converter and a subsequent digital filter. The use of two filters is necessary to reduce the dimensions of the control problem by only taking into account the first eight natural modes in the horizontal plane. However, they introduce a phase lag of about 60 ms at a sampling frequency of 200 Hz; this delay must be taken into account when designing the controller.

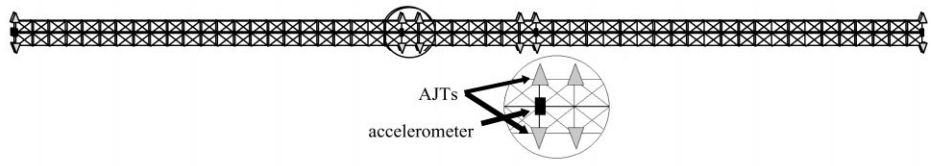

Fig. 2. Actuator and sensor positions — top view.

2.2. Mathematical model

The linear mathematical model of the structure, used for the design of the controller and obtained with a finite element analysis, is as follows:

$$\mathbf{q}(t) = \mathbf{\Phi}\eta(t), \tag{1}$$

$$\ddot{\eta}(t) + 2\mathbf{\Xi\Omega}\dot{\eta}(t) + \mathbf{\Omega}^2\eta(t) = \mathbf{\Phi}^{\mathrm{T}}\mathbf{f}(t), \tag{2}$$

$$\mathbf{y}(t) = \mathbf{M}_{\mathrm{s}}\ddot{\mathbf{q}}(t), \tag{3}$$

$$\mathbf{y}(t) = -\mathbf{M}_{\mathrm{s}}\mathbf{\Phi\Omega}^2\eta(t) - 2\mathbf{M}_{\mathrm{s}}\mathbf{\Phi\Xi\Omega}\dot{\eta}(t) + \mathbf{M}_{\mathrm{s}}\mathbf{\Phi\Phi}^{\mathrm{T}}\mathbf{M}_{\mathrm{a}}\mathbf{u}(t), \tag{4}$$

where $\mathbf{q}$ is the vector of the physical Cartesian co-ordinates of the truss nodes, η is the vector of the amplitudes of the vibration modes, $\mathbf{\Phi}$ is the matrix of the modal shape vectors and $\mathbf{\Omega}$ and $\mathbf{\Xi}$ are the matrices of natural frequencies and damping coefficients. $\mathbf{\Omega}$ and $\mathbf{\Xi}$ are diagonal because the natural modes are uncoupled. $\mathbf{M}_{\mathrm{s}}$ transforms $\mathbf{q}$ into the vector of sensor displacements, thus depends on the position and orientation of the accelerometers, whereas $\mathbf{M}_{\mathrm{a}}$ indicates the influence of the control vector $\mathbf{u}$ on the structure and thus depends on actuator positioning. $\mathbf{y}$ is the vector of acceleration measurements. Natural frequencies and damping coefficients for the first eight modes are indicated in Table 1.

Omitting, for conciseness, the time dependence of the state, input and output vectors, Eqs. (1)–(4) can be rearranged into the standard form

$$\dot{\mathbf{x}} = \mathbf{A}\mathbf{x} + \mathbf{B}\mathbf{u}, \tag{5}$$

$$\mathbf{y} = \mathbf{C}\mathbf{x} + \mathbf{D}\mathbf{u}, \tag{6}$$

where

$$\mathbf{x} = \begin{bmatrix} \eta \\ \dot{\eta} \end{bmatrix}, \quad \mathbf{A} = \begin{bmatrix} 0 & \mathbf{I} \\ -\mathbf{\Omega}^2 & -2\mathbf{\Xi\Omega} \end{bmatrix}, \quad \mathbf{B} = \begin{bmatrix} 0 \\ -\mathbf{\Phi}^{\mathrm{T}}\mathbf{M}_{\mathrm{a}} \end{bmatrix}, \tag{7}$$

$$\mathbf{C} = [-\mathbf{M}_{\mathrm{s}}\mathbf{\Phi\Omega}^2 - 2\mathbf{M}_{\mathrm{s}}\mathbf{\Phi\Xi\Omega}], \quad \mathbf{D} = \mathbf{M}_{\mathrm{s}}\mathbf{\Phi\Phi}^{\mathrm{T}}\mathbf{M}_{\mathrm{a}}, \tag{8}$$

where $\mathbf{x} \in \Re^{16}$, from which a discrete-time model can be obtained by means of a standard sampling transformation.

It is easily verified that system (5), (6) is completely controllable and observable.

Table 1
Natural frequencies and damping coefficients

Mode	f (Hz)	ζ
Rigid rotation	0.2928	0.0032
Rigid translation	0.3117	0.0085
I bending	1.0324	0.0139
II bending	2.9302	0.0110
III bending	5.5359	0.0110
IV bending	8.7808	0.0100
V bending	12.8800	0.0100
VI bending	17.6991	0.0100

The aim of the control system is to damp the vibrations of the first six natural modes in the horizontal plane, which includes two rigid modes and four bending modes.

The controller requires the state variables of the system, which are not directly accessible. The state estimator used is a Kalman state prediction filter, designed in a previous project (Casella et al., 1996), which estimates the first eight natural modes. This work concentrates on the design of the control law implementing a sliding mode (or variable structure) controller.

3. Sliding mode control theory

3.1. Introduction

In this section only the most important features of variable structure control (VSC) and the sliding mode will be introduced with reference to linear, time-invariant plants. For a more detailed presentation of VSC, the reader is referred to Utkin (1978) and DeCarlo, Zak and Matthews (1988).

Sliding mode (or variable structure) control is basically a control law that switches rapidly between two values or gains, with the objective of bringing the system's state-space trajectory onto a specified surface.

The general VSC problem is stated for a system represented by the state equation

$$\dot{\mathbf{x}} = \mathbf{A}\mathbf{x} + \mathbf{B}\mathbf{u}, \tag{9}$$

where $\mathbf{x} \in \Re^n$ and $\mathbf{u} \in \Re^m$. VSC design consists in finding:

(1) m switching functions, represented in vector form as $\sigma(\mathbf{x})$, and
(2) a variable structure control law

$$u_i(\mathbf{x}) = \begin{cases} u_i^+ & \text{when } \sigma_i(\mathbf{x}) > 0, \\ u_i^- & \text{when } \sigma_i(\mathbf{x}) < 0, \end{cases} \quad i = 1, \cdots, m, \tag{10}$$

so that the reaching modes satisfy the "reaching condition", namely, reach the set $\sigma(\mathbf{x}) = 0$ (switching surface) in finite time.

The meaning of the above statement is as follows:

(1) Design a switching surface $\sigma(\mathbf{x}) = 0$ to represent a desired system dynamics;
(2) Design a variable structure control law $u_i(\mathbf{x})$ so that any state $\mathbf{x}$ outside the switching surface is driven to reach the surface in finite time. On the switching surface the sliding mode takes place, following the desired system dynamics. In this way the overall VSC system is globally asymptotically stable.

The overall VSC system, for which the switching surface and the control have been properly designed, has the following characteristics:

(a) Since the origin of the phase plane represents the equilibrium state of the system, the sliding mode represents the behaviour of the system during the transient period. In other words, the surface (or line) that describes $\sigma(\mathbf{x}) = 0$ defines the transient response of the system during the sliding mode.
(b) During the sliding mode, trajectory dynamics are of a lower order than the original model.
(c) During the sliding mode, system dynamics are solely governed by the parameters that describe the line $\sigma(\mathbf{x}) = 0$.

3.2. Sliding surface design

In order to illustrate the surface design techniques used in this project the co-ordinate transformation

$$\tilde{\mathbf{x}} = \mathbf{T}\mathbf{x} \tag{11}$$

is defined with which the original system is transformed to "regular form", where

$$\mathbf{T}\mathbf{B} = \begin{bmatrix} \mathbf{0} \\ \hat{\mathbf{B}} \end{bmatrix} \tag{12}$$

in which the matrix $\hat{\mathbf{B}}$ of dimension $m \times m$ is non-singular. The behaviour of system (1) in the transformed state-space variables is described by the equations

$$\dot{\tilde{\mathbf{x}}}_1 = \hat{\mathbf{A}}_{11}\tilde{\mathbf{x}}_1 + \hat{\mathbf{A}}_{12}\tilde{\mathbf{x}}_2, \tag{13}$$

$$\dot{\tilde{\mathbf{x}}}_2 = \hat{\mathbf{A}}_{21}\tilde{\mathbf{x}}_1 + \hat{\mathbf{A}}_{22}\tilde{\mathbf{x}}_2 + \hat{\mathbf{B}}\mathbf{u}, \tag{14}$$

where $\tilde{\mathbf{x}}_1$ and $\tilde{\mathbf{x}}_2$ are vectors consisting, respectively, of the first $(n - m)$ and the last m components of the vector $\tilde{\mathbf{x}}$, and the $\hat{\mathbf{A}}_{ij}$ are block matrices that derive from the partitioning of the matrix $\mathbf{T}\mathbf{A}\mathbf{T}^{-1}$. Note that if the number of control variables in system (5)–(8) is the same as the number of natural modes to be controlled, then $\mathrm{T} = \mathrm{I}$.

Without loss of generality, the sliding surface $\sigma(\tilde{\mathbf{x}})$ is supposed to be linear, i.e. having the form

$$\sigma(\tilde{\mathbf{x}}) = \hat{\mathbf{C}}\tilde{\mathbf{x}} = \hat{\mathbf{C}}_1\tilde{\mathbf{x}}_1 + \hat{\mathbf{C}}_2\tilde{\mathbf{x}}_2, \tag{15}$$

where

$$\mathbf{C}\mathbf{T}^{-1} = [\hat{\mathbf{C}}_1\ \hat{\mathbf{C}}_2]. \tag{16}$$

On the sliding surface $\sigma(\tilde{\mathbf{x}}) = 0$, which implies that $\hat{\mathbf{C}}_1\tilde{\mathbf{x}}_1 + \hat{\mathbf{C}}_2\tilde{\mathbf{x}}_2 = 0$, or equivalently

$$\tilde{\mathbf{x}}_2 = -\hat{\mathbf{C}}_2^{-1}\hat{\mathbf{C}}_1\tilde{\mathbf{x}}_1 = -\hat{\mathbf{F}}\tilde{\mathbf{x}}_1. \tag{17}$$

Substituting (17) in (13) the plant description during the sliding motion becomes

$$\dot{\tilde{\mathbf{x}}}_1 = (\hat{\mathbf{A}}_{11} - \hat{\mathbf{A}}_{12}\hat{\mathbf{F}})\tilde{\mathbf{x}}_1, \tag{18}$$

$$\tilde{\mathbf{x}}_2 = -\hat{\mathbf{F}}\tilde{\mathbf{x}}_1. \tag{19}$$

It is thus clear that the problem of designing a system with desirable properties in the sliding mode can be regarded as a state feedback design problem. It will be assumed, in what follows, that $\hat{\mathbf{C}}_2 = \mathbf{I}$. Thus, the sliding surface is determined by $\hat{\mathbf{C}}_1$.

The sliding surface can be designed in different ways, for example using standard linear feedback design techniques, such as eigenvalue placement or quadratic minimisation techniques, in all of which the vector $\tilde{\mathbf{x}}_2$ plays the role of the control vector, and $\hat{\mathbf{F}} = \hat{\mathbf{C}}_2^{-1}\hat{\mathbf{C}}_1$ plays the role of feedback gain matrix.

The sliding surface $\mathbf{S}$ is finally determined by (Dorling & Zinober, 1986)

$$\mathbf{S} = \hat{\mathbf{B}}^{-1}[\hat{\mathbf{F}}\ \ \mathbf{I}]\mathbf{T}. \tag{20}$$

As the control design is based on a simplified nominal system, to avoid control spillover caused by the unmodelled parts of the plant, it is desirable that the closed-loop system be robust, in the sense that its closed-loop poles be as insensitive to perturbations as possible.

3.3. Application to the control of structures

In the experiments on the space structure, after designing the sliding surface by quadratic minimisation, different robust pole assignment techniques were used (Kautsky, Nichols & Van Dooren, 1985; Tits & Yang, 1996). Results obtained by numerical simulations with the different techniques, not reported for conciseness, showed that robust pole assignment strategies did not significantly improve the closed-loop system's robustness and caused a loss of information concerning the single

controlled mode dynamics (Allen, 1996). Therefore, the technique chosen for sliding surface design is quadratic minimisation (Utkin & Yang, 1978). The interested reader is referred to Allen (1996) for a deeper analysis of the effects of the design parameters on the system performances.

The cost functional to be minimised is

$$\boldsymbol{J} = \frac{1}{2}\int_0^\infty \tilde{\eta}^{\mathrm{T}}\mathbf{Q}\tilde{\eta}\,\mathrm{d}t, \tag{21}$$

where the matrix $\mathbf{Q} > 0$ is diagonal, and $\tilde{\eta}$ is the vector of the vibration modes to be controlled, i.e.

$$\tilde{\eta} = [\eta_1 \ldots . \eta_6 \dot{\eta}_1 \ldots . \dot{\eta}_6]^{\mathrm{T}}. \tag{22}$$

The surface is designed with four, not six, control variables, thus controlling conjunctly actuators n°s 2, 3 and n°s 4, 5 (see Fig. 2). This strategy has again been selected on the basis of numerical simulations. In this way the sliding surface design is simplified, and unnecessary fuel consumption, caused by adjacent actuators being switched on in opposite directions, is avoided.

The diagonal matrix $\mathbf{Q}$ determines the relative weights which are imposed on the state variables while designing the sliding surface. Experimental results show that the matrix $\mathbf{Q}$ shapes the closed-loop natural mode dynamics. The weights are determined first by analysis of the results of the simulations and then fine tuned experimentally, so that the different mode dynamics are comparable. In particular, the bending modes are weighted about 10 times more heavily than the rigid modes, as (a) the rigid modes are determined by the suspension system and would be completely different in a real space-borne structure, and (b) the integral of the acceleration signal caused by the rigid modes is usually much greater than the one due to the bending modes, because of the differences in frequencies and damping factors; thus if the bending modes were not weighed more heavily the controller would be relatively insensible to the bending modes and concentrate on damping the rigid modes. It will be shown in the experimental results that the damping of the rigid body modes is very efficient even with this choice of the matrix $\mathbf{Q}$.

3.4. Chattering reduction

In order to avoid unnecessary chattering, a dead-band must be introduced. In principle the dead band could be defined on the local velocity, but not withstanding the resulting complications it is defined on the sliding surface.

This choice is motivated by the following considerations, illustrated in Figs. 3 and 4, in which simulation results of a lightly damped second-order (spring-mass) system are reported.

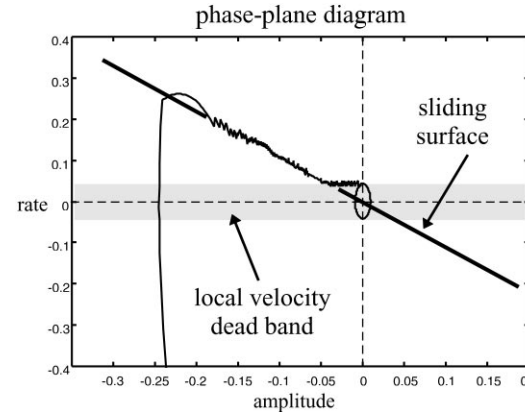

Fig. 3. Dead-band on local velocity with sliding mode.

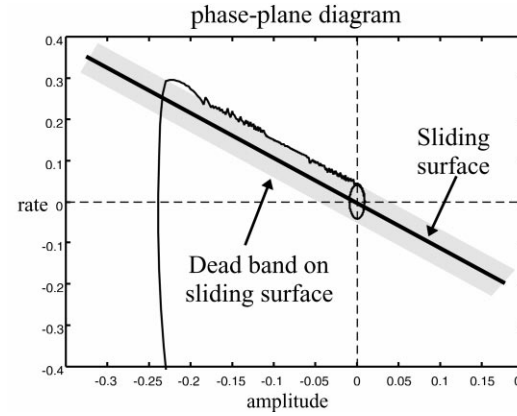

Fig. 4. Dead-band on sliding surface.

The dead-band defined on local velocity not only does not reduce chattering during the sliding mode but also interferes with the control law, which tries to keep the system on the sliding surface. Thus, the overall effect is not a reduction but an increase in the amount of chattering in the final stages of control.

The sliding mode with a dead-band on the sliding surface is thus not ideal, and can be referred to as a quasi-sliding mode (Hung, Gao & Hung, 1993). The control law becomes

$$u_i = \begin{cases} -1 & \text{when} \quad \sigma_i(\tilde{\eta}) < -\varepsilon_i, \\ 0 & \text{when} \quad -\varepsilon_i \leqslant \sigma_i(\tilde{\eta}) \leqslant \varepsilon_i, \\ 1 & \text{when} \quad \sigma_i(\tilde{\eta}) > \varepsilon_i. \end{cases} \tag{23}$$

The problem is the determination of the width of the dead-band: if the width is too small there is a lot of useless and expensive chattering causing high fuel consumption; if the dead band is too wide the control is less effective and there is a lot of residual motion. A compromise must be found. Difficulties arise due to the fact that the dead-band is defined on the switching surface, and not on local velocity.

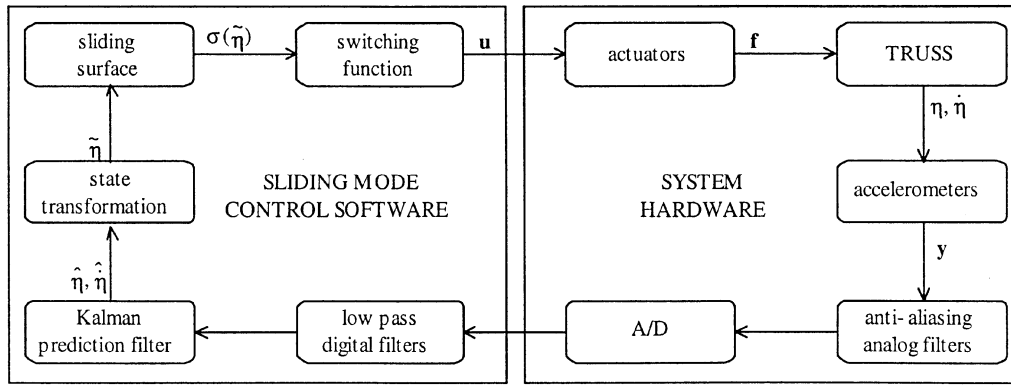

Fig. 5. Overall SMC scheme.

The problem was solved in the following way: an acceptable amount of residual movement was determined for every natural mode (in terms of speed: 2.5 mm/s), thus determining $\tilde{\eta}_0$.

Once the sliding surface has been determined, the corresponding dead-band width is determined by the relationship

$$\mathbf{S}\tilde{\eta}_0 = \bar{\varepsilon}. \tag{24}$$

sliding surface is

$$\mathbf{Q} = \begin{bmatrix} 0.7\mathbf{I} & \mathbf{0} \\ \mathbf{0} & \mathrm{diag}(\mathbf{q}) \end{bmatrix} \quad \text{with}$$

$$\mathbf{q} = [0.4 \;\; 0.5 \;\; 4.0 \;\; 6.5 \;\; 8.0 \;\; 1.8]. \tag{25}$$

The resulting sliding surface and dead-band are defined as

$$\mathbf{S} = \begin{bmatrix} 0.29 & 0.12 & -0.11 & 2.06 & 13.71 & -16.84 & 0.26 & 0.16 & -0.59 & 0.66 & 0.54 & -0.35 \\ 0.31 & 0.14 & 0.32 & 2.12 & 11.76 & -21.56 & 0.29 & 0.16 & 0.50 & -0.71 & 0.44 & -0.50 \\ -0.31 & 0.14 & 0.32 & -2.12 & 11.76 & 21.56 & -0.29 & 0.16 & 0.50 & 0.71 & 0.44 & 0.50 \\ -0.29 & 0.12 & -0.11 & -2.06 & 13.71 & 16.84 & 0.26 & 0.16 & -0.59 & -0.66 & 0.54 & 0.35 \end{bmatrix}, \tag{26}$$

The dead-band width is subsequently adjusted following extensive simulation and experimentation and considering the natural symmetry of the structure.

3.5. Overall control scheme

The complete control system diagram is sketched in Fig. 5. where the relevant functional blocks are highlighted and the flow of data traced with reference to Eqs. (1)–(24).

4. Experimental results

In this paragraph the experimental results will be presented and compared with the results presented in a previous study (Casella et al., 1996) in which a local velocity control law (velocity sign with elastic switch-off) was implemented, with the aim of damping the first four bending modes only.

As previously discussed, the first six modes are controlled (two rigid body and four bending modes), using four control variables; the weight matrix **Q** designing the

$$\bar{\varepsilon} = [0.0104 \;\; 0.0105 \;\; 0.0102 \;\; 0.0102 \;\; 0.0105 \;\; 0.0104]. \tag{27}$$

The initial conditions for the experiments are set using an electromagnetic shaker connected to one end of the structure, which brings the truss to a steady oscillation via excitation at one or a combination of its natural frequencies. The shaker is automatically disconnected when the predetermined initial condition is reached.

The diagrams refer to the modal variables and local velocity estimated by the Kalman state prediction filter.

The first result shown refers to the control of the second rigid-body mode, and proves the effect of the control system despite the relatively low weight assigned to the mode in the design of the controller. Fig. 6 shows the response of the truss, in terms of tip velocity, with and without control. The damping enhancement is evident. No further detail will be given on this test, since it can not be compared to other control methods.

For the control of the bending modes, the initial conditions have been kept equal to those of past experiments (Casella et al., 1996) to allow a direct comparison of the results. They are reported in Table 2, and the most notable results will be discussed.

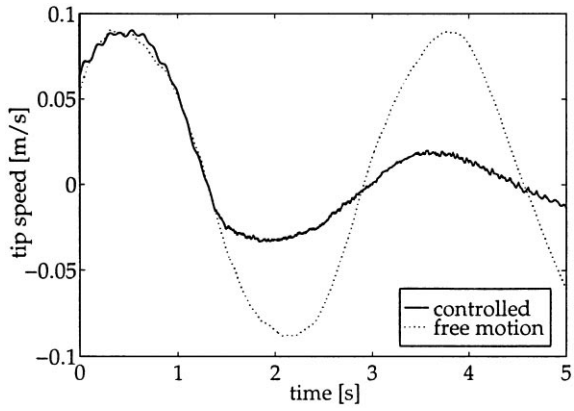

Fig. 6. Sliding mode control of second rigid mode.

Results obtained by excitation at the system's first and second natural bending frequency are reported respectively in Figs. 7 and 8.

In these figures, starting from the upper left and going in a clockwise direction, the following significant parameters are reported: (a) the tip speed in the free motion and controlled case; (b) the tip control force; (c) the phase plane diagram of the controlled bending mode; and (d) the phase plane diagram of the free oscillation. In particular, Figs 7(a) and (b) and 8(a) and (b) are considered to be representative of the overall behaviour of the truss. Moreover in Figs. 7(c) and 8(c) in the controlled phase-plane diagram, motion on the sliding surface is evident. Also the dead-band on the sliding surface is evident: the system is not kept exactly on the sliding surface, but is very close as the dead-band is quite small, and barely visible in the diagram.

The successful design of the controller is evident from the phase-plane portraits, which converge to the origin much more rapidly in the controlled case. As stated by the theory (Eq. (23)), the controller is designed on the basis of the phase-plane behaviour of the structure, which unfortunately has a poor physical meaning. The well-behaved phase plane diagram of Figs. 7(c) and 8(c) finds its physical equivalent in the highly damped time histories of the truss nodes positions, reported in Figs. 7(a) and 8(a), and the velocities and accelerations.

In order to verify the performances in the case of a more complex disturbance, in Fig. 9 the results achieved by exciting the truss in a combination of the first four bending modes are reported. These results confirm the previous conclusions and demonstrate the effectiveness of the proposed controller.

4.1. Comparison with VSES control law experimental results

As was mentioned earlier the results obtained with sliding mode control were compared with the best experimental results previously obtained on the same experimental structure (Casella et al., 1996).

VSES control law is basically a modified velocity-sign control law. Two modifications were introduced: the control law is inhibited when the control force is greater and opposite to the elastic force acting on the structure, and a local velocity dead-band is added to avoid persistent control action in the vicinity of the origin, thus switching off control action when the local velocity determined by the bending modes is less than 2.5 mm/s.

The resulting control law is then defined, as shown in Fig. 10, on the a_{el}–v plane instead of the x–v plane, where $a_{el} = -kx/m$ is the elastic acceleration due to the spring force and $a_c = f_{max}/m$ is the acceleration due to the control force.

This control law aims to damp the first four bending modes only: the local velocity needed for the calculation of the control values is obtained by considering the estimated bending modes only. Reported experimental results differ from Casella, Locatelli and Schiavoni (1996) as in this paper the velocity considering all modes is reported, not just bending modes.

The initial conditions and the state prediction filter are the same as in sliding mode experimental results.

Numerical results concerning total fuel consumption, maximum tip speed when the control action is definitely completed and the times required for the controller to completely damp the vibrations obtained with the two control strategies are summarised in Table 3.

Table 2
Initial conditions for the experiments

	Participation of each mode to initial tip velocity (m/s)			
Disturbed modes	I bending	II bending	III bending	IV bending
I bending	0.25	—	—	—
II bending	—	0.25	—	—
I–IV bending	0.12	0.12	0.12	0.03

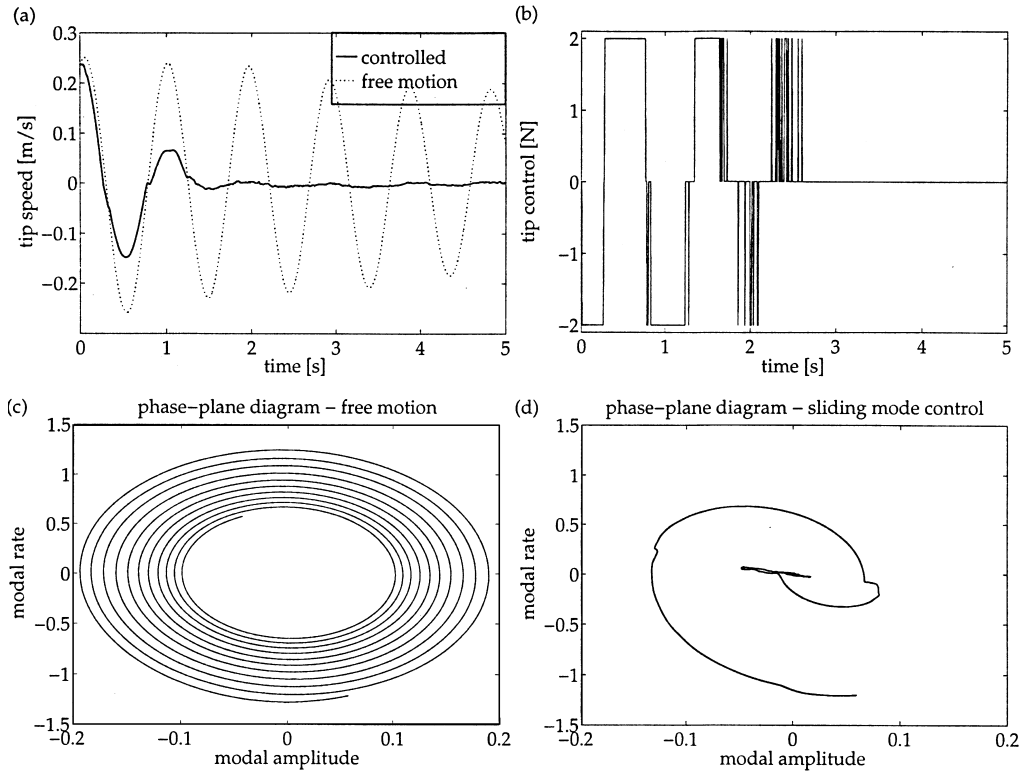

Fig. 7. Sliding mode control of first bending mode.

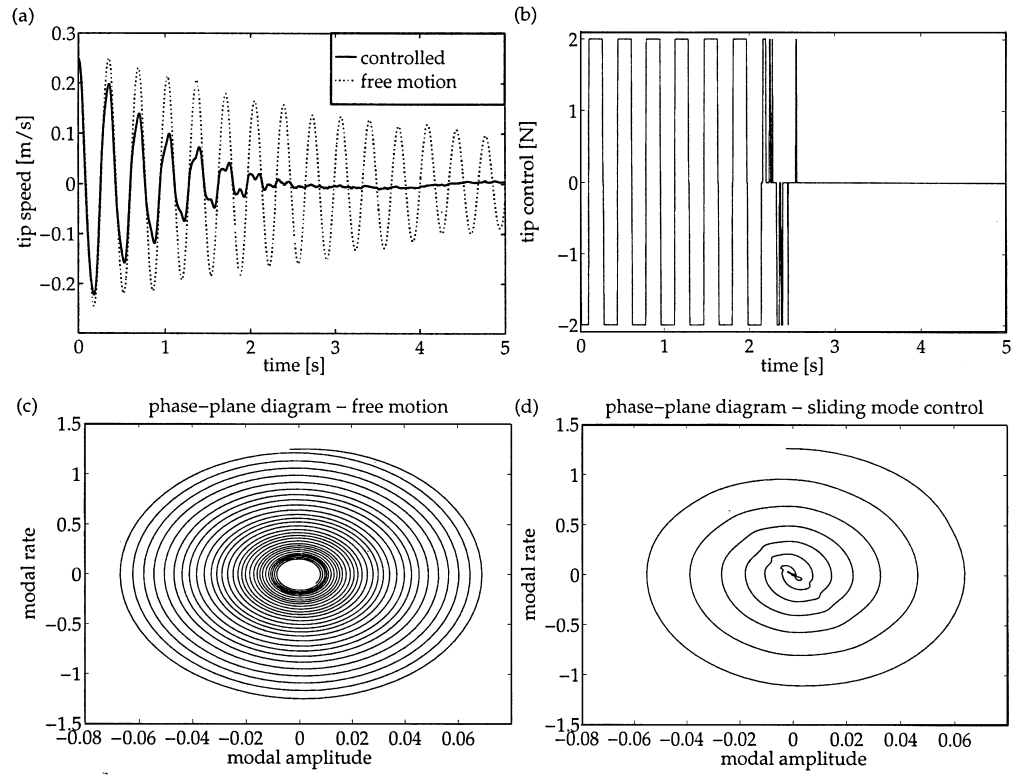

Fig. 8. Sliding mode control of second bending mode.

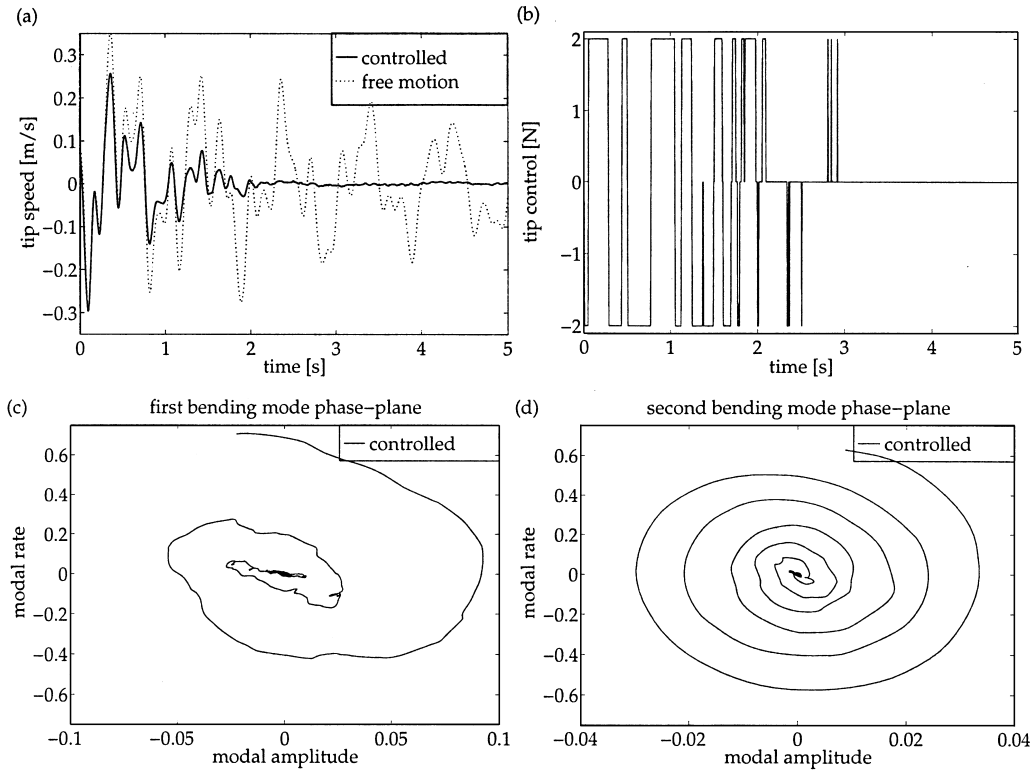

Fig. 9. Sliding mode control of combined first four bending modes.

Table 3
Experimental results

	Fuel consumption (s)		Residual speed (mm/s)		Control time (s)	
	SMC	VSES	SMC	VSES	SMC	VSES
I bending mode	9.14	7.49	6	19	2.7	4.5
II bending mode	13.78	10.2	8	15	2.6	3
I–IV bending modes	11.18	7.69	6	16	2.9	4.5

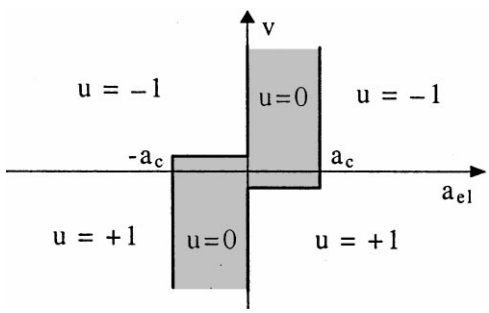

Fig. 10. Definition of VSES control.

Examination of the graphical and numerical results reported in the diagrams (see Figs. 11 and 12) and in Table 3 allows the following conclusions to be drawn.

Sliding mode control is more effective than VSES control, as the full control force is used until the system can be kept on the sliding surface (compare tip control during excitation at the first bending frequency). Thus control time, that is the time necessary to bring the truss to rest is much smaller for sliding mode control. The higher residual speed with VSES control is caused by motion due to the rigid modes that are excited during the control action and not damped. The higher fuel consumption observed with sliding mode control is caused by two different actions: in the first place, by rigid mode control, as rigid modes are unintentionally excited during both excitation and during control action and thus must be damped, causing high fuel consumption because of the higher inertia; also, as control is more efficient and lasts a shorter time, the system's natural damping contributes less, thus active control must be greater.

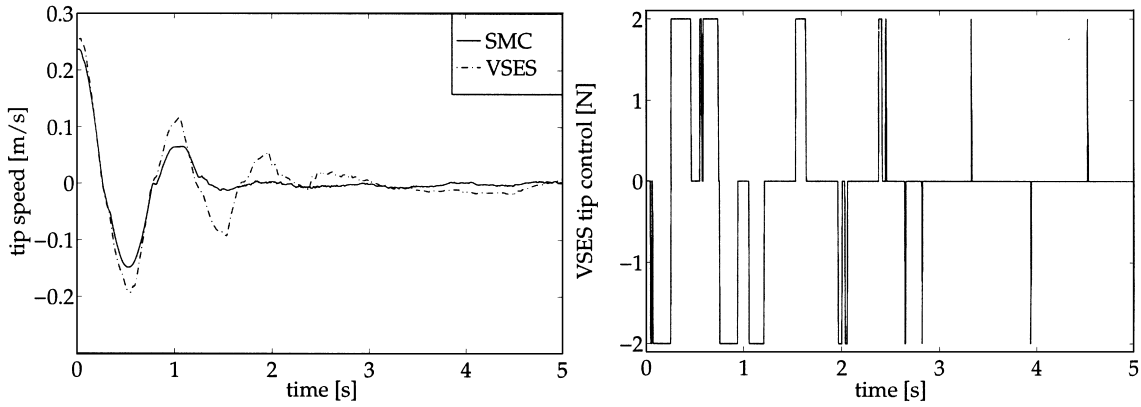

Fig. 11. SMC and VSES control of first bending mode.

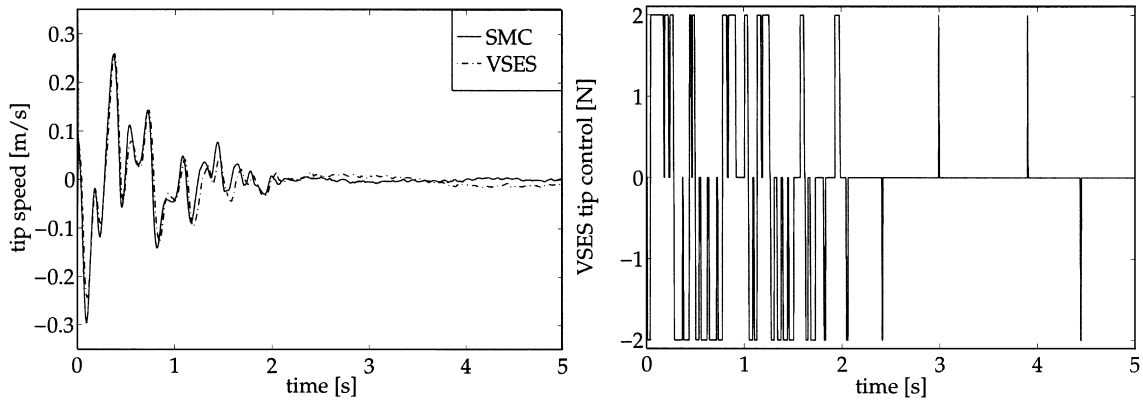

Fig. 12. SMC and VSES control of combined first four bending modes.

5. Conclusion

Experimental results have confirmed that the control strategy based on sliding modes is a very effective technique for vibration suppression in flexible space structures. Excellent results have been obtained not withstanding the presence of a state observer. Also its feasibility for the design of a controller for complex systems has been verified experimentally.

The truss has also been equipped with three pairs of piezoelectric active members (PAMs) which allow control modulation. The great design flexibility which characterises sliding mode control allows this control strategy to be applied to many different problems. Thus, for the near future a new project is planned for the design of a sliding mode controller that employs both AJTs and PAMs, thus combining the use of on/off and modulating actuators and providing higher control power and an increased chattering reduction.

Acknowledgements

This study has been supported by ASI grants No. ARS-96-192 and No. 94-RS-54. The authors gratefully acknowledge the helpful suggestions and technical support provided by F. Casella.

References

Allen, M. (1996). Sliding mode control of a large space structure. M.S. graduation thesis, Italy: University of Pavia, Pavia (in Italian).

Bernelli-Zazzera, F. (1995). Design of a sliding mode controller for vibration suppression of a LSS laboratory model. *Proceedings of the Xth VPI & SU symposium on structural dynamics and control* (pp. 501–512) Virginia: Blacksburg.

Casella, F., Locatelli, A., & Schiavoni, N. (1996). Nonlinear controllers for vibration suppression in a large flexible structure. *Control Engineering Practice*, *4*(6), 791–806.

DeCarlo, R. A., Zak, S. H., & Matthews, G. P. (1988). Variable structure control of nonlinear multivariable systems: A tutorial. *Proceedings of the IEEE*, *76*(3), 212–232.

Dodds, S.J., & Senior, M. (1993). A sliding mode approach to the simultaneous shape and attitude control of flexible space structures with uncertain dynamics. In C. L. Kirk & P. C. Hughes (Editors), *Dynamics and control of structures in space II* (pp. 257–277). Computational Mechanics Publications.

Dorling, C. M., & Zinober, A. S. I. (1986). Two approaches to hyperplane design in multivariable variable structure control systems. *International Journal of Control*, *44*(1), 65–82.

Ercoli-Finzi, A., Gallieni, D., Ricci, S., Design, modal testing and updating of a large space structure laboratory model. *Proceedings of the IXth VPI&SU symposium on dynamics and control of large structures* (pp. 409–420). Virginia: Blacksburg.

Hallauer, W. L., & Lamberson, S. (1989). Experimental active vibration damping of a plane truss using hybrid actuation. *Proceedings of the 30th structures, structural dynamics and materials conference* (pp. 80–90). Alabama: Mobile.

Hung, J. Y., Gao, W., & Hung, J. C. (1993). Variable structure control: A survey. *IEEE Transactions on Industrial Electronics*, *40*(1), 2–21.

Junkins, J. L., Mechanics and control of large flexible structures. *Progress in astronautics and aeronautics*. Washington, DC: American Institute of Aeronautics and Astronautics.

Kautsky, J., Nichols, N. K., & Van Dooren, P. (1985). Robust pole assignment in linear state feedback. *International Journal of Control*, *41*(5), 1129–1155.

Sparks Jr., D. W., & Juang, J.-N. (1992). Survey of experiments and experimental facilities for control of flexible structures. *Journal of Guidance, Control and Dynamics*, *15*(4), 801–816.

Tits, A. L., & Yang, Y. (1996). Globally convergent algorithms for robust pole assignment by state feedback. *IEEE Transactions on Automatic Control*, *41*(10), 1432–1452.

Utkin, V. I. (1977). Variable structure systems with sliding modes. *IEEE Transactions on Automatic Control*, *AC-22*(2), 212–222.

Utkin, V. I. (1978). *Sliding modes and their application in variable structure systems*. Moscow: Mir.

Utkin, V. I., & Yang, K. D. (1978). Methods for constructing discontinuity planes in multidimensional variable structure systems. *Automation and Remote Control*, *39*, 1466–1470.